Correction of PMT position effect for a lead-scintillating fiber electromagnetic calorimeter*

LI Zu-Hao(李祖豪)[1,2;1)] WANG Ling-Yu(王玲玉)[1] XU Wei-Wei(许伟伟)[1,2]
CHEN Guo-Ming(陈国明)[1] LÜ Yu-Sheng(吕雨生)[1] CHEN He-Sheng(陈和生)[1]

[1] Institute of High Energy Physics, Chinese Academy of Sciences, Beijing 100049, China
[2] Graduate University of Chinese Academy of Sciences, Beijing 100049, China

Abstract: The position effect of the photoelectron multiplier tube (PMT) of the electromagnetic calorimeter (ECAL) of Alpha Magnetic Spectrometer-02 (AMS-02) has been studied with beam-test data. The reconstructed deposited energy in a layer versus incidence position in the cell can be described by Gaussian distribution, maximum and minimum value can be obtained when the particle passes across the center and the edge of a cell respectively. The distribution can be used to correct the effect of incidence position on energy reconstruction. Much better energy resolution was acquired be got with the correction, for 100 GeV electrons, energy resolution improved from 3% to 2%.

Key words: electromagnetic calorimeter, photo multiplier tube, position effect, energy resolution

PACS: 29.40.Vj **DOI:** 10.1088/1674-1137/37/2/026201

1 Introduction

The Alpha Magnetic Spectrometer-02 (AMS-02) is a particle physics detector designed to search antimatter and dark matter as well as to measure the primary cosmic ray precisely in space [1]. It was launched onto the International Space Station (ISS) on 15th May, 2011 and will run on board for 10 to 20 years. The electromagnetic calorimeter (ECAL) of AMS-02 is a fine grained lead-scintillating fiber sampling calorimeter which allows for precise, 3-dimensional imaging of the longitudinal and lateral shower development. The system provides a high electron/hadron discrimination, as well as good energy and angular resolution [2, 3]. The structure of ECAL and the beam-test setup are briefly described in Section 2.

The gain of the PMT used by AMS-02 ECAL is non-uniform with position which leads to different outputs for the same amount of energy deposited in different positions in the ECAL. To get a better energy resolution, the incidence position effect was studied with beam-test data and correction for the effect was applied(Section 3).

2 AMS-02 ECAL and beam test

The calorimeter consists of a pancake composed of 9 super-layers for an active area of 648 mm× 648 mm and a thickness of 166.5 mm. Each super-layer is 18.5 mm thick and made of 11 grooved 1 mm thick lead foils interleaved with layers of 1 mm diameter scintillating fibers, glued together with epoxy resin. The detector imaging capability is obtained by stacking super-layers with fibers alternately parallel to the x-axis (4 layers) and y-axis (5 layers) (Fig. 1(a)). Each super-layer is read out by 36 photo multiplier tubes (PMTs), arranged alternately

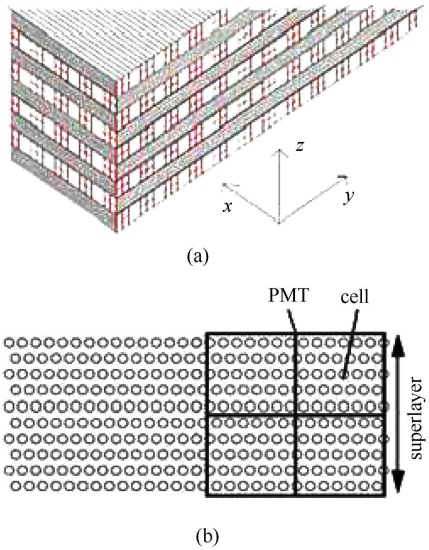

Fig. 1. Structure of AMS-02 ECAL. (a) The superlayer assembly; (b) The structure of a portion of a superlayer with one PMT.

Received 6 March 2012, Revised 26 March 2012
∗ Supported by National Natural Science Foundation of China (10805050)
1) E-mail: lizh@ihep.ac.cn

on the two opposite ends. Fibers are read out, on one end only, by four anode Hamamatsu R700-00-M4 PMTs, with each anode covering an active area of 9 mm×9 mm, corresponding to 35 fibers, defined as a cell (Fig. 1(b)), the minimum detection unit. A more detailed description of the ECAL can be found in Refs. [2, 3].

The fight model of the ECAL was successfully tested and calibrated on the H4 Beam-Line of the Super Proton Synchrotron (SPS) at CERN in July 2007. The schematic plot of the beam test setup is shown in Fig. 2. The whole model was mounted on a rotating table which can move along x and y axes and can rotate around z axes. Events were triggered by four crossed plastic scintillating counters. Three silicon tracker ladders were installed in front of the ECAL, which can provide accurate information of the beam incident position. Data were taken with 100 GeV proton beam and 6 GeV to 250 GeV electron beam. Incidence angles were 0, 4.5, 7.5 and 15 degrees. A more detailed introduction to the setup of the beam test is described in Ref. [4].

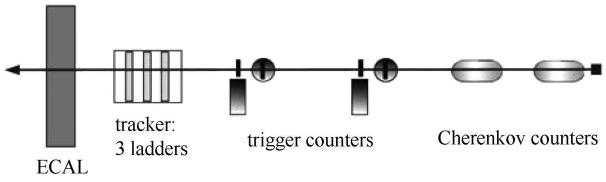

Fig. 2. The AMS-02 ECAL beam test setups.

3 Incidence position effect and correction

The PMT used by AMS-02 ECAL has four anodes, the size of the PMT is 18 mm×18 mm, each anode is 9 mm×9 mm. The gain of the PMT is non-uniform with position as shown in Fig. 3 [5]. The gain is lower at the edge of the anode(which corresponds to the edge and the center of the PMT), and higher in the central part of the anode. For each cell of ECAL covered by an anode, scintillating light created by the fiber located in the central part of a cell will be guided to the central part of an anode, which leads to higher output signal for the same amount of energy deposited in the central part of a cell than those at the edge of a cell.

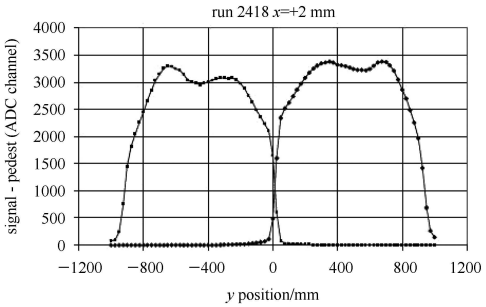

Fig. 3. PMT gain vs. position.

From the result of Monte Carlo Simulation as shown in Fig. 4, lateral distribution of deposited energy in a layer is quite narrow, thus total output of deposited energy in a layer mainly depends on three cells near the axis of the electromagnetic shower, especially the central cell which the axis passes across.

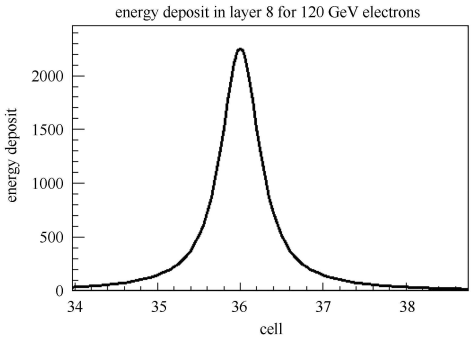

Fig. 4. Lateral distribution of deposited energy (The unit of x axis is the cell width=9 mm).

For the reason described above (non-uniform of gain with position and narrow lateral distribution of deposited energy), when the axis of an electromagnetic shower passes across the central part of a cell, the output signal of deposited energy in the layer will be higher than those across the edge of a cell. We tried to check this with beam-test data and found a way to correct it.

The raw data of the AMS-02 ECAL are the ADC values for each cell. The ADC values can be converted to format with energy unit by calibration with formula $E_{\rm cell}={\rm ADC}_{\rm cell}/{\rm Cal}_{\rm cell}$. $E_{\rm cell}$ represents the output of deposited energy in the cell, ${\rm ADC}_{\rm cell}$ and ${\rm Cal}_{\rm cell}$ represent the ADC values and calibration factors of the cell. The calibration of the AMS-02 ECAL is described in Ref. [6]. The total output of deposited energy in a layer which is named as $E_{\rm layer}$ is the sum of $E_{\rm cell}$ for all the cells in the layer.

Two examples of the plots of $E_{\rm layer}$ values versus beam position inside the cell from beam-test data, from the eighth and the 13th layers of 100 GeV electrons, are shown in Fig. 5(a) and Fig. 5(b). The circle points with dotted curve and the squares with solid curve represent the results from data with 0 and 15 degrees incidence angle respectively. The x axis is the beam position inside the cell with the unit of cell width (9 mm).

It is proved from the plots that $E_{\rm layer}$ values are higher when the incidence position is located in the center of a cell, lower when in the edge. The distribution of $E_{\rm layer}$ values versus beam position inside the cell can be roughly described by Gaussian distribution. The maximum difference of $E_{\rm layer}$ for a given layer depends on the magnitude of σ of the Gaussian fitting.

As shown in Fig. 5, $E_{\rm layer}$ values from inclined events are roughly equal to the values from a perpendicular event. Smaller difference is due to the difference of track length.

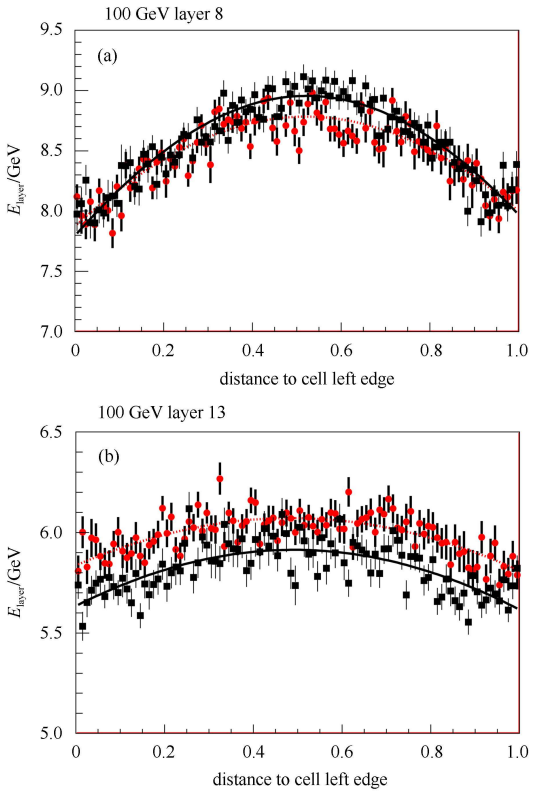

Fig. 5. $E_{\rm layer}$ versus beam position inside cell. The circle points with dotted curve and the squares with solid curve represent the results from data with 0 and 15 degrees incidence angle respectively, (a) for the eighth layer and (b) for 13th layer.

The longitudinal distribution of deposited energy for an electromagnetic shower can be described as Γ function [7], deposited energy in a layer increases with layer number before the shower-max, then decreases with layer number. For AMS-02 ECAL, the shower-max for 100 GeV electrons is reached at about the 9th layer, so $E_{\rm layer}$ increases with the layer number before the 9th layer, and decreases after the 9th layer. For events with 15 degrees incidence angle, the total track length in the ECAL will be longer, the 8th and 13th layers are roughly equivalent to the 8.3th and 13.5th layers of the perpendicular one respectively, thus the reconstructed energy in the 8th layer for inclined events is a little higher than the perpendicular events, but a little lower in the 13th layer. The σ values from Gaussian fitting for inclined events are a little higher than the perpendicular events for a given layer, but the difference is very small. This is the reason why $E_{\rm layer}$ for inclined events is higher in the central part but smaller near the edge for the result of the 8th layer.

σ values from Gaussian fitting of plots like Fig. 5 vary with the layer number, an example from 250 GeV electrons is shown in Fig. 6. The unit of σ values in Fig. 6 is the cell width (9 mm). It is shown from the plots in Fig. 6 that from the 4th layer to 15th layers (corresponding to 3.6 radiation length X_0 to $14.5X_0$), σ value increases linearly with the layer number. Similar plots can be obtained for electrons with all the other energy.

For the first three layers, the electromagnetic shower is just beginning, thus very little energy is deposited, which means the contribution to the final result of energy reconstruction is very limited; for the last several layers, the σ values are more than 2. The maximum differences of reconstructed energy for different incidence position are less than 3%, the correct facts for position effect are smaller, and variation on σ has limited effect on the final reconstructed result. For the reason described above, the σ value for the first three layers and last layers can be substituted by the value extrapolated from the linear function fitting from the central part of the plot.

The intercept and the slope from a linear fitting on the plots in Fig. 6 with the range of 4 to 15 layers are named $P1$ and $P2$ respectively. $P1$ and $P2$ vary with beam momentum as shown in Fig. 7. $P1$ increases roughly linearly with momentum. $P2$ can be described by exponential plus constant function of momentum.

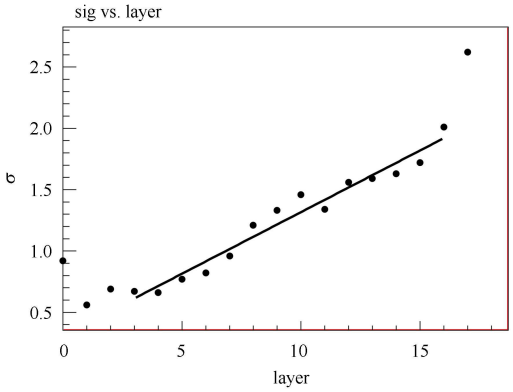

Fig. 6. σ value vs. layer number. The unit of σ is cell width (9 mm).

The correction on position effect is done by the following steps:

1) Calculate $E_{\rm layer}$ values for all layers by sum $E_{\rm cell}=ADC_{\rm cell}/Cal_{\rm cell}$ for all the cells in the layer;

2) Calculate a preliminary reconstructed total energy without position effect correction [8];

3) Reconstruct incidence positions x for each layer;

4) Calculate $P1$ and $P2$ from preliminary reconstructed energy by linear and exponential plus linear function respectively with parameters acquired from fitting on plots in Fig. 7;

5) Calculate σ values for each layer from the layer number by linear function with parameter $P1$ and $P2$;

6) Calculate corrected $E_{\rm layer\_corr}$ for each layer from formula $E_{\rm layer\_corr}=E_{\rm layer}/{\rm e}^{-(x-0.5)^2/\sigma^2}$

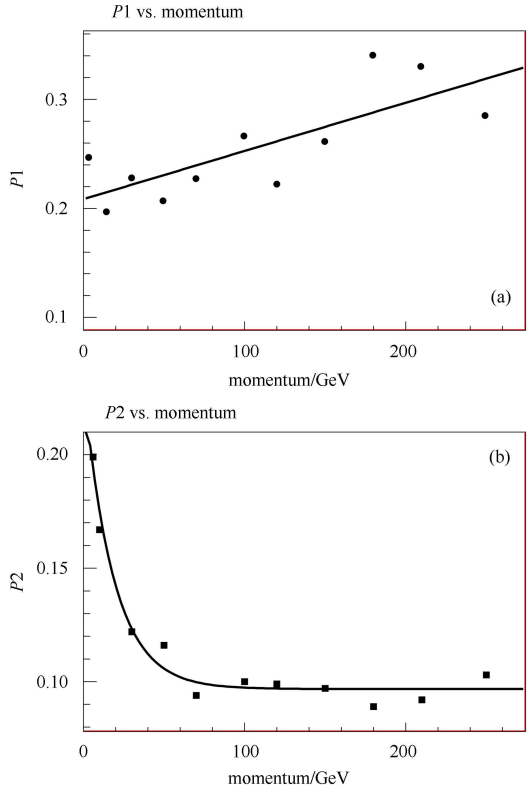

Fig. 7. $P1$, $P2$ vs. momentum.

4 Results and conclusions

We apply the correction on position effect by using methods described above for deposited energy in each layer for perpendicular electrons with 11 different energies, then correct the longitudinal leakage with the last layer method described by Ref. [8]. Energy resolutions for electrons with different momenta are plotted in Fig. 8. For 100 GeV electrons, energy resolution has been improved from $\sim 3\%$ to $\sim 2\%$, a significant improvement made by the correction of position effect.

Electrons with five different energies and three different incidence angles from the beam-test had been analyzed, longitudinal leakage had been corrected with the last layer method described by Ref. [8], and position effect corrected with the method mentioned above. The longitudinal leakage and position effect correction are same for electrons with the same energy but different incidence angles. Reconstructed energies are listed in Table 1. The linearity of reconstructed energy is better than 0.5% as shown in Table 1.

Energy resolutions are listed in Table 2 from which it can be seen that energy resolutions are a little better for bigger incidence angles, but there are not too many differences.

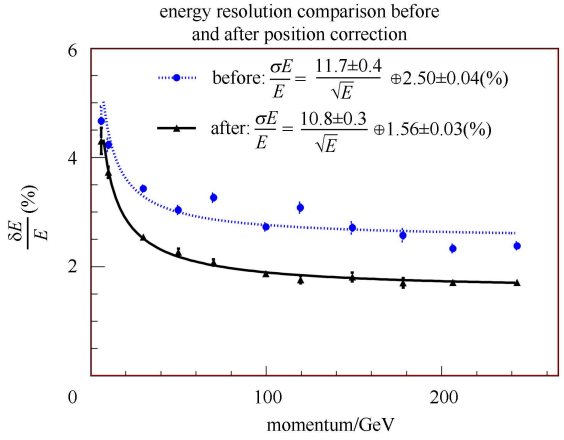

Fig. 8. Comparison of energy resolutions with and without the position effect correct. The circle points with dotted curve and the triangles with solid curve represent the results with and without position effect correction respectively.

Table 1. Reconstructed energy for different energy and incidence angle.

$E_{\rm beam}$/GeV	10.0	30.0	99.7	149.0	243.0
$E_{\rm rec0}$/GeV	10.0	30.1	100.0	149.2	243.8
$E_{\rm rec7.5}$/GeV	10.0	29.8	99.5	149.4	244.3
$E_{\rm rec15}$/GeV	10.0	30.0	100.2	149.5	243.5

Table 2. Energy resolution for different energy and incidence angle.

$E_{\rm beam}$/GeV	10.0	30.0	99.7	149.0	243.0
${\rm Res}_{\rm rec0}(\%)$	3.80	2.57	1.84	1.72	1.63
${\rm Res}_{\rm rec7.5}(\%)$	3.60	2.51	1.70	1.60	1.53
${\rm Res}_{\rm rec15}(\%)$	3.49	2.45	1.73	1.56	1.46

In conclusion, the method for position effect correction described above is independent of the incidence angle; significant improvements on energy resolution can be obtained by applying position effect correction with the method.

References

1 Battiston R et al. Astropart. Phys., 2000, **13**: 51–74
2 Antonelli M et al. Nuclear Physics B, 1977, **54**: 14–19
3 Cadoux F et al. Nuclear Physics B, 2002, **113**(Proc.Suppl.): 159–165
4 Di Falco Stefano. Advances in Space Research, 2010, **45**(1): 112–122
5 Kossakowski R et al. AMSNote-2002-01-03
6 LI Zu-Hao et al. HEP & NP, 2004, **28**: 521–525 (in Chinese)
7 Longo E, Sestili I. Nuclear Instrument Methods, 1975, **128**: 283
8 LI Zu-Hao et al. HEP & NP, 2004, **28**: 1182–1188 (in Chinese)